TITLE

Morphological changes in functional tricuspid regurgitation on contrast-enhanced computed tomography correlates to tricuspid regurgitation grade

AUTHORS

Hiroki Uchiyama [1*], Ryo Harada [1], Takuma Mikami [1], Naomi Yasuda [1], Yosuke Kuroda [1], Shuichi Naraoka [1], Takeshi Kamada [1], Atsuko Muranaka [2], Keishi Ogura [3], Kazutoshi Tachibana [4], Koichi Osuda [5], Nobuyoshi Kawaharada [1]

[1] Department of Cardiovascular Surgery, Sapporo Medical University, Sapporo, Japan; [2] Department of Cardiovascular, Renal and Metabolic Medicine, Sapporo Medical University, Sapporo, Japan; [3] Division of Radiology and Nuclear Medicine, Sapporo Medical University Hospital, Sapporo, Japan; [4] Department of Cardiovascular Surgery, Hakodate Goryoukaku Hospital, Hakodate, Japan; [5] Division of Radiology, Hakodate Goryoukaku Hospital, Hakodate, Japan

[*] Corresponding author: Hiroki Uchiyama, Department of Cardiovascular Surgery, Sapporo Medical University, Minami 1-jo Nishi 16-chome, Chuo-ku, Sapporo, Hokkaido, 060-8543, Japan. E-mail: hirouchiyama@sapmed.ac.jp

ABSTRACT

PURPOSE: To examine the relationship between each severity of functional tricuspid regurgitation (FTR) and morphological evaluation on contrast-enhanced computed tomography (CT).

METHODS: Forty-five patients underwent contrast-enhanced CT. Tricuspid annulus area (TAA), tricuspid annulus circumference (TAC), right ventricular volume (RVV), and the distances between the tips and bases of the papillary muscles were measured on contrast-enhanced CT in diastole and systole. The patients were classified ~~organized~~ into 4 groups by TR grade measured by transthoracic echocardiography (none+trivial: 26, mild: 6, moderate: 6, severe: 7), and the data were compared among the groups.

RESULTS: In parameters measured on contrast-enhanced CT images, TAA, TAC, and the distances between the tips of the anterior and posterior papillary muscles in both diastole and systole and RVV in diastole were significantly different among the groups ($p<0.05$). Parameters that had correlations with TR grade were TAA, TAC, RVV and the distances between the tips of the anterior and posterior papillary muscles in both diastole and systole ($r>0.40$). The septal papillary muscle could not be identified in about 1/3 (35.6%) of cases.

CONCLUSIONS: TAA, TAC, RVV, and the distance between the tips of the anterior and posterior papillary muscles measured on contrast-enhanced CT images had relatively positive correlations with TR grade.

Keywords:
Functional tricuspid regurgitation; Contrast-enhanced computed tomography; Tricuspid annulus area; Tricuspid annulus circumference; Right ventricular volume

TEXT

Introduction

Functional tricuspid regurgitation (FTR) occurs from morphological changes of the tricuspid valve complex that develop secondary to tricuspid annulus dilation and ventricular enlargement because of volume or pressure overload of the right ventricle due to left heart disease, such as valvular failure [1-5]. FTR severity is diagnosed by transthoracic echocardiography and estimated semiquantitatively using the range or area of the regurgitant jet[1]. Transthoracic echocardiography is performed easily, and a past study evaluated morphological changes of the tricuspid valve complex by transthoracic echocardiography [6]. However, transthoracic echocardiography has some limitations, such as the need for the evaluator to have experience and limited ultrasound examination by ribs or air.

On the other hand, contrast-enhanced computed tomography (CT) is also performed easily and is useful for morphological assessment. Recently, detailed preoperative morphological assessment using contrast-enhanced CT has become possible, for example, for transcatheter aortic valve implantation (TAVI) [7-9]. However, few papers have considered morphological assessment of FTR using contrast-enhanced CT.

We postulated that, in FTR, morphological changes of tricuspid annulus area (TAA), tricuspid annulus circumference (TAC), right ventricular volume (RVV), and the distance between papillary muscles could be identified on contrast-enhanced CT images. The aim of this study was to evaluate the morphological changes in FTR cases using contrast-enhanced CT.

Materials and methods

Study population

Between April 2018 and July 2019, 45 patients planned for cardiovascular surgery underwent contrast-enhanced CT and transthoracic echocardiography. Patients who had primary tricuspid regurgitation, de novo myocardial infarction within less than 28 days, unstable angina, end-stage renal failure, infective endocarditis, active hemorrhagic diseases (gastrointestinal bleeding, trauma, etc.), or postoperative pacemaker implantation were excluded. This study was approved by the research ethics committee of Sapporo Medical University.

The 45 cases were divided into 4 groups by TR grade measured by transthoracic echocardiography (none+trivial: 26 cases, mild: 6 cases, moderate: 6 cases, severe: 7 cases), and then differences among groups were examined. The correlations of TR grade and contrast-enhanced CT measurements were also examined.

Contrast-enhanced computed tomography

ECG-gated 320-detector-row multislice computed tomography (Aquilion one, Toshiba Medical Systems, Tokyo, Japan) was used for this study. In order to ensure that the tricuspid annulus and right ventricle would be clearly depicted, very early phase images were taken.

The reconstructed volume data images were transferred to OsiriX (Pixmeo, Geneva, Switzerland) and Ziostation2 (Ziosoft, Tokyo, Japan). TAA, TAC, RVV, and the distances between papillary muscles (anterior, posterior, and septal, and each distance of tips [t] and bases [b]) were measured on contrast-enhanced CT images. Each was measured at diastole (d) and at systole (s). For example, the distance between the tips of the anterior and posterior papillary muscles is shown as dtAP. Figure 1 shows the measurements.

Transthoracic echocardiography

A Philips iE33 (Koninklijke Philips N.V., Amsterdam, Netherlands) was used for this study. General measurements, TR grade, and tricuspid annulus diameter (TA, end-diastole, 4-chamber view) were measured.

Statistical analysis

One-way ANOVA was performed to evaluate the mean differences among the four groups, and $p<0.05$ was considered significant. When significant differences were found, the multiple comparison method was used to examine differences between groups; when the parameter could be assumed to have equal dispersion, the Tukey method was used, and when not, the Games-Howell method was used. Pearson's correlation coefficient was calculated between groups, and $p<0.05$ was considered significant. In addition, all cases were divided into the non FTR group (none + trivial + mild) and the FTR group (moderate + severe), and risk factors for FTR ≥ moderate were evaluated by multiple logistic regression analysis. The dependent variable was FTR ≥ moderate or not, and the independent variables were age, body surface area, diastolic and systolic TAA, TAC, RVV, and the distances between the tips and bases of the anterior and posterior papillary muscles, which were measurable in all cases. Independent variables were chosen by the variable increase method (likelihood ratio). All statistical analyses were performed using IBM SPSS Statistics version 25.0 (IBM, Armonk, NY, USA).

Results

Table 1 shows the patients' characteristics and parameters measured on contrast-enhanced CT images and transthoracic echocardiography for every TR grade. Age and body surface area did not show significant differences.

As for TAA, TAC, and RVV measured on contrast-enhanced CT images, dTAA, sTAA, dTAC, sTAC, and dRVV showed significant differences among the groups ($p<0.01$). Figures 2, 3, and 4 show box-and-whisker plots and correlations with the TR grade of TAA, TAC, and RVV. All parameters had correlations with TR grade ($r>0.5$).

With respect to the distances between papillary muscles measured on contrast-enhanced CT images, dtAP, stAP, dbAP, dtPS, dbPS, and sbPS showed significant differences among the groups ($p<0.05$).

In addition, as a subgroup analysis, all cases were divided into the non FTR group (none + trivial + mild) and the FTR group (moderate + severe), and risk factors for FTR ≥ moderate were evaluated by multiple logistic regression analysis (Table 2). Risk factors were selected by the variable increase method (likelihood ratio), and the only risk factor identified was sTAA, with an odds ratio of 1.77 [95% confidence interval 1.26-2.49].

Discussion

TAA, TAC, and RVV measured on contrast-enhanced CT images had relatively positive correlations with the TR grade measured by transthoracic echocardiography, showing that tricuspid annulus dilation and ventricular enlargement are causes of FTR progression. Furthermore, the correlation coefficients of dTAA, sTAA, dTAC, sTAC, and dRVV were higher than the correlation coefficient of TA measured by transthoracic echocardiography (r=0.624), and it appeared that parameters measured on contrast-enhanced CT images had stronger correlations with TR grade than TA measured by transthoracic echocardiography.

With respect to the distances between papillary muscles, dtAP, dbAP, and stAP showed significant differences among the groups, and dtAP had a particularly positive correlation with TR grade (r=0.484). Although it is not as related as TAA, TAC, and RVV, it is thought that tAP tends to expand as FTR becomes severe.

In about 1/3 (35.6%) of cases, the septal papillary muscle could not be identified on contrast-enhanced CT. According to autopsy reports, cases with many small septal papillary muscles or tendinous cords that appear directly from the septal walls of the right ventricle have been described, and there are many variations of septal papillary muscles [10)]. The present study was similar, and there were many cases in which septal muscles could not be identified because of the many variations. Anterior and posterior papillary muscles were identified in all cases; only the distance of the anteroposterior papillary muscles could be measured effectively. In some cases, the posterior papillary muscle was also small, and only the anterior papillary muscle was clearly visible, so it is thought that the anterior papillary muscle contributes most to the tricuspid valve.

On multiple logistic regression analysis as a subgroup analysis, sTAA contributed most to FTR ≥ moderate. This is because tricuspid regurgitation occurs during systole, and it is thought that sTAA contributes to FTR. Generally, the tricuspid annulus is measured in end-diastole by transthoracic echocardiography, but one study pointed out that the tricuspid annulus should be measured in systole [11)], with which we agree. Measurement of tricuspid annulus diameter and determination of ring size should be done in systole.

Kabasawa et al. also evaluated FTR by contrast-enhanced CT [12)] in 35 patients who underwent contrast-enhanced CT, and end-diastolic and end-systolic tricuspid valve annular diameters (TVADs), tethering angles, and tethering height were significantly correlated with preoperative TR severity. The result for the tricuspid annulus was similar to that of the present study, and the present study did not evaluate tethering angles and tethering height, but evaluated the distances between papillary muscles and right ventricular volume.

In comparison with sonography, contrast-enhanced CT is slightly more invasive because of the use of contrast media and radiation exposure. However, contrast-enhanced CT is useful because it can perform morphological evaluations, especially quantitative measurement, objectively and in detail. In the present study, the detailed morphological assessment of FTR was possible using contrast-enhanced CT.

The present study has some limitations. First, we did not evaluate the change over time for each patient. We will evaluate the morphological changes and surgical indications for FTR in the future.

Secondly, the tricuspid annulus actually has three-dimensional geometry [13, 14]. However, in the present study, the true annulus structure might not been evaluated, because the tricuspid annulus was measured in a section of contrast-enhanced CT.

Thirdly, the present study depended mainly on morphological examination on contrast-enhanced CT, and other aspects of the cases were not considered. For example, there has been a report that a huge left atrium or atrial fibrillation is a risk factor for late TR after surgery[15], and further studies are needed to evaluate patients' status in greater detail.

Conclusions

TAA, TAC, RVV, and the distances between papillary muscles (especially tAP), measured on contrast-enhanced CT images, had relatively positive correlations with TR grade measured by transthoracic echocardiography.

Detailed morphological assessment of functional tricuspid regurgitation is possible using contrast-enhanced CT.

REFERENCES

[1] Baumgartner H, Falk V, Bax JJ, Bonis MD, Hamm C, Holm PJ, Lung B, Lancellotti P, Lansac E, Monoz DR, Rosenhek R, Sjögren J, Mas PT, Vahanian A, Walther T, Wendler O, Windecker S, Zamorano JL. 2017 ESC/EACTS Guidelines for the management of valvular heart disease. European Heart Journal 2017;38:2739-2791.

[2] Chuwa T, Pilgrim JP, Shah PM, Ormiston JA, Wong M. The tricuspid valve annulus: study of size and motion in normal subjects and in patients with tricuspid regurgitation. Circulation 1982;66:665-671.

[3] Ubago JL, Figueroa A, Ochoteco A, Colman T, Duran RM, Duran CG. Analysis of the amount of tricuspid valve annular dilatation required to produce functional tricuspid regurgitation. Am J Cardiol 1983;52:155-158.

[4] Sagie A, Schwammenthal E, Padial LR, Vazquez de Prada JA, Weyman AE, Levine RA. Determinants of functional tricuspid regurgitation in incomplete tricuspid valve closure: doppler color flow study of 109 patients. J Am Coll Cardiol 1994;24:446-453.

[5] Dreyfus GD, Corbi PJ, Chan KM, Bahrami T. Secondary tricuspid regurgi- tation or dilatation: which should be the criteria for surgical repair? Ann Thorac Surg 2005;79:127-132.

[6] Spinner EM, Lerakis S, Higginson J, Pernetz M, Howell S, Veledar E, Yoganathan AP. Correlates of tricuspid regurgitation as determined by 3D echocardiography: pulmonary arterial pressure, ventricle geometry, annular dilatation, and papillary muscle displacement. Circ Cardiovasc Imaging 2012;5:43-50.

[7] Bloomfield GS, Gillam LD, Hahn RT, Kapadia S, Leipsic J, Lerakis S, Tuzcu M, Douglas PS. A practical guide to multimodality imaging of transcatheter aortic valve replacement. J Am Coll Cardiol Img 2012;5:441-455.

[8] Ribeiro HB, Webb JG, Makkar RR, Cohen MG, Kapadia SR, Kodali S, Tamburino C, Barbanti M, Chakravarty T, Jilaihawi H, Paradis JM, Brito FS, Cánova SJ, Cheema AN, Jaegere PP, Valle R, Chiam PTL,Moreno R, Pradas G, Ruel M, Salgado-Fernández J, Sarmento-Leite R, Toeg HD, Velianou JL, Zajarias A, Babaliaros V, Cura F, Dager AE, Manoharan G, Lerakis S, Pichard AD, Radhakrishnan S, Perin MA, Dumont E, Larose E, Pasian SG, Nombela-Franco L, Urena U, Tuzcu EM, Leon MB, Amat-Santos IJ, Leipsic J, Rodés-Cabau J. Predictive factors, management, and clinical outcomes of coronary obstruction following transcatheter aortic valve implantation. J Am Coll Cardiol 2013;62:1552-1562.

[9] Latsios G, Spyridopoulos TN, Toutouzas K, Synetos A, Trantalis G, Stathogiannis K, Penesopoulou V, Oikonomou G, Brountzos E, Tousoulis D. Multi-slice CT (MSCT) imaging in pretrans-catheter aortic valve implantation (TAVI) screening. How to perform and how to interpret. Hellenic Journal of Cardiology 2018;59:3-7.

[10] Silver MD, Lam JHC, Ranganathan N, Wigle ED. Morphology of the human tricuspid valve. Circulation 1971;Mar;43(3):333-348.

[11] Calafiore A, Iaco AL, Romeo A, Scandura S, Meduri R, Varone E. Echocardiographic-based treatment of functional tricuspid regurgitation. J Thorac Cardiovasc Surg 2011;142:308-313.

[12] Kabasawa M, Kohno H, Ishizaka T, Ishida K, Funabashi N, Kataoka A, Matsumiya G. Assessment of functional tricuspid regurgitation using 320-detector-row multislice computed tomography: Risk factor analysis for recurrent regurgitation after tricuspid annuloplasty. Thorac Cardiovasc Surg 2014;147:312-320.

[13] Fukuda S, Saracino G, Matsumura Y, Daimon M, Tran H, Greenberg NL, Hozumi T, Yoshikawa J, Thomas JD, Shiota T. Three-dimensional geometry of the tricuspid annulus in healthy subjects and in patients with functional tricuspid regurgitation: a real-time, 3-dimensional echocardio- graphic study. Circulation 2006;114(suppl):I-492-I-498.

[14] Rogers JH, Bolling SF. The Tricuspid Valve Current Perspective and Evolving Management of Tricuspid Regurgitation. Circulation 2009;119:2718-2725

[15] Matsuyama K, Matsumoto M, Sugita T, Nishizawa J, Tokuda Y, Matsuo T. Predictors of residual tricuspid regurgitation after mitral valve surgery. Ann Thorac Surg 2003;75:1826-1828.

FIGURES

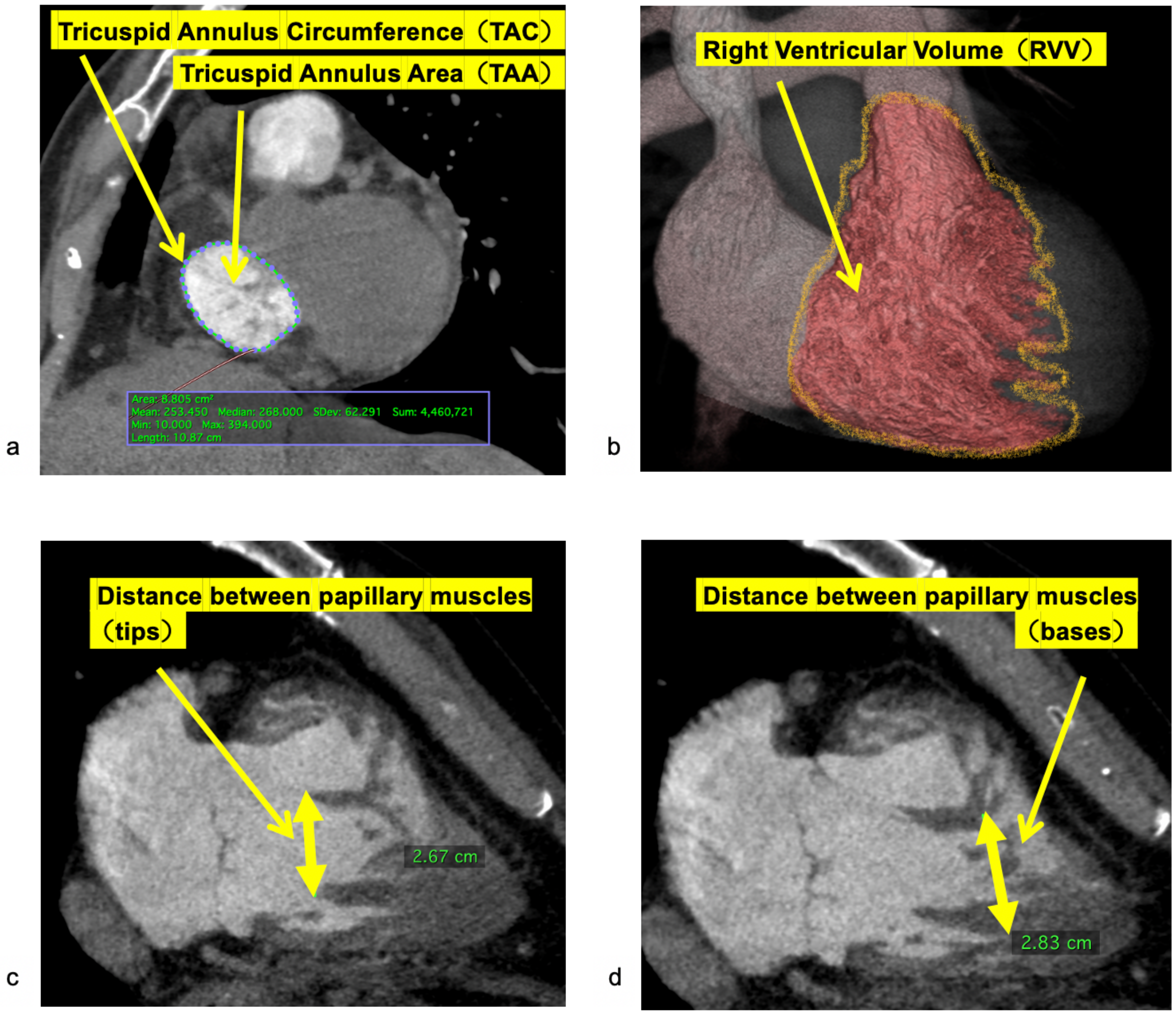

Figure 1. a) Tricuspid annulus area and tricuspid annulus circumference, b) Right ventricular volume, c) Distance between papillary muscles (tips), d) Distance between papillary muscle (bases)

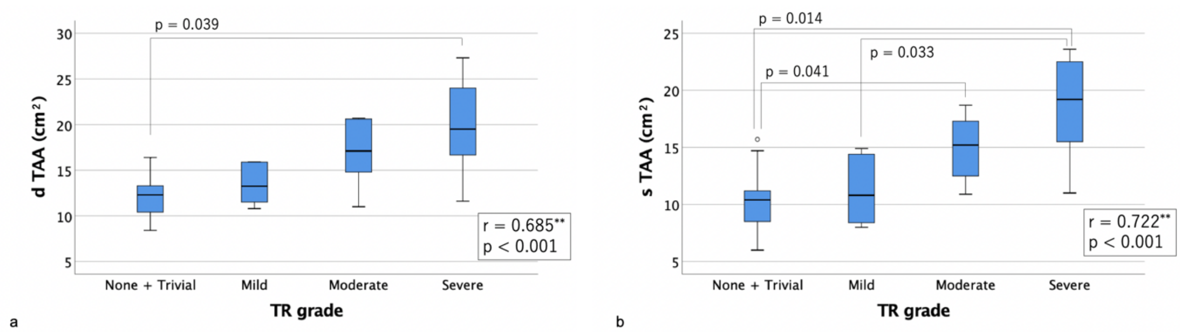

Figure 2. Box-and-whisker plots of diastolic (a) and systolic (b) tricuspid annulus area

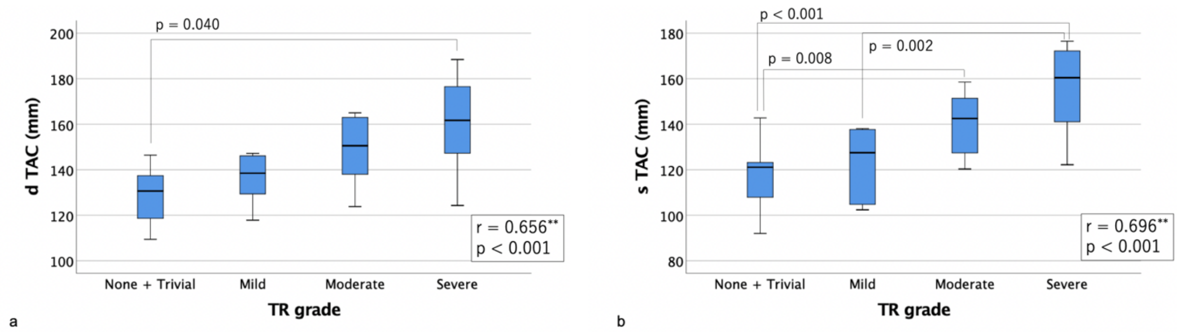

Figure 3. Box-and-whisker plots of diastolic (a) and systolic (b) tricuspid annulus circumference

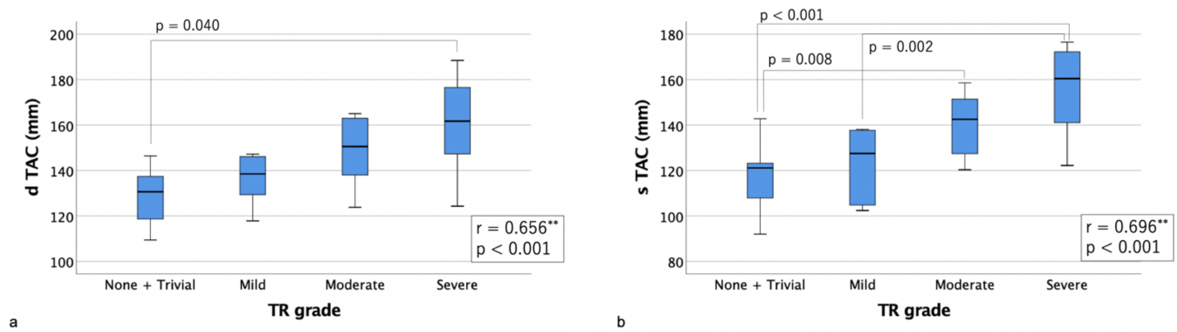

Figure 4. Box-and-whisker plots of diastolic (a) and systolic (b) right ventricular volume

TABLES

Table 1. Patient's characteristics and parameters measured on contrast- enhanced CT and transthoracic echocardiography

	All cases (n=45)	None + Trivial (n=26)	Mild (n=6)	Moderate (n=6)	Severe (n=7)	p value	r	p value of r
Age (y)	73.2±9.5	72.0±11.4	72.5±6.2	76.3±4.0	75.4±7.5	0.699	0.167	0.272
Body height (cm)	160.5±8.5	160.7±8.0	159.4±10.2	161.5±7.0	159.8±11.3	0.971	-0.022	0.887
Body weight (kg)	58.8±10.1	59.4±8.6	57.2±12.2	56.2±6.5	60.5±16.2	0.782	-0.013	0.931
Body surface area (cm^2)	1.61±0.16	1.62±0.14	1.58±0.18	1.59±0.098	1.62±0.26	0.909	-0.027	0.862
Enhanced CT								
dTAA (cm^2)	14.2±4.3	12.2±2.2*	13.4±2.2	16.9±3.8	20.0±5.6*	0.012	0.685	<0.001
sTAA (cm^2)	12.3±4.3	10.2±2.3*,**	11.2±3.0†	15.0±3.1**	18.5±4.9*,†	0.003	0.772	<0.001
dTAC (mm)	137.4±18.1	128.9±11.0*	136.2±11.4	148.5±16.6	160.3±22.9*	<0.001	0.656	<0.001
sTAC (mm)	127.2±20.2	117.7±12.5*,**	123.0±15.8†	140.5±14.9**	155.1±21.4*,†	<0.001	0.696	<0.001
dRVV (mL)	161.5±77.7	129.6±38.0*	118.5±27.3†	197.6±53.5	286.1±97.9*,†	0.003	0.704	<0.001
sRVV (mL)	108.6±59.0	86.1±29.9*	93.1±34.2	139.4±66.0	178.8±89.9*	0.074	0.582	<0.001
dtAP (mm)	26.0±5.2	23.7±4.4*,**	28.0±2.0	29.5±7.0**	29.4±4.2*	0.005	0.484	0.001
stAP (mm)	19.9±4.8	18.1±4.7*	21.3±2.0	21.8±6.1	23.4±2.9*	0.024	0.433	0.003
dbAP (mm)	29.4±6.8	27.5±5.9*	32.5±4.3	28.3±11.1	35.0±3.9*	0.015	0.348	0.019
sbAP (mm)	24.5±6.1	23.0±5.7	27.3±3.7	23.3±8.3	28.3±6.0	0.122	0.271	0.071
dtPS (mm)	20.2±5.2	17.5±2.6*	21.1±4.5	19.9±4.0	26.1±6.4*	0.001	0.622	<0.001
stPS (mm)	15.3±4.6	13.6±2.7	18.7±2.8	13.2±2.9	19.3±6.4	0.185	0.443	0.016
dbPS (mm)	25.5±7.7	21.7±6.1*	27.3±6.7	28.7±9.3	30.9±7.0*	0.031	0.516	0.003
sbPS (mm)	20.6±6.1	18.6±4.2*	20.8±9.8	18.2±7.0	26.5±5.8*	0.02	0.472	0.010
dtSA (mm)	32.8±5.0	32.3±3.9	27.2±1.0	33.1±4.3	36.2±6.6	0.057	0.297	0.105
stSA (mm)	25.1±5.0	25.7±3.9	23.5±1.9	26.0±7.8	28.1±6.2	0.63	0.189	0.325
dbSA (mm)	36.1±7.7	35.2±6.7	31.7±4.6	36.9±7.5	39.5±10.5	0.466	0.228	0.218
sbSA (mm)	28.3±6.1	28.7±5.2	25.8±4.7	26.6±7.5	29.0±8.3	0.858	-0.014	0.942
Transthoracic echocardiography								
TA (mm)	31.4±5.7	28.7±4.6*	30.0±2.4**	32.4±3.4	38.7±6.3*,**	0.001	0.624	<0.001

dTAA: diastolic tricuspid annulus area

sTAA: systolic tricuspid annulus area

dTAC: diastolic tricuspid annulus circumference

sTAC: systolic tricuspid annulus circumference

dRVV: diastolic right ventricular volume sRVV: systolic right ventricular volume

dtAP: diastolic anterior-posterior papillary muscles distance (tips)

stAP: systolic anterior-posterior papillary muscles distance (tips)

dbAP: diastolic anterior-posterior papillary muscles distance (basal)

sbAP: systolic anterior-posterior papillary muscles distance (basal)

dtPS: diastolic posterior-septal papillary muscles distance (tips)

stPS: systolic posterior-septal papillary muscles distance (tips)

dbPS: diastolic posterior-septal papillary muscles distance (bases)

sbPS: systolic posterior-septal papillary muscles distance (bases)

dtSA: diastolic septal-anterior papillary muscles distance (bases)

stSA: systolic septal-anterior papillary muscles distance (bases)

dbSA: diastolic septal-anterior papillary muscles distance (bases)

sbSA: systolic septal-anterior papillary muscles distance (bases)

TA: tricuspid annulus diameter (4-chamber view, diastolic)

*,**,†: significant difference in $p<0.05$ between groups

Table 2. Multivariable analysis for FTR ≥ moderate

Variable	Odds ratio	95% CI	p value
sTAA (cm^2)	1.77	1.26-2.49	0.001

sTAA: systolic tricuspid annulus area

和文抄録

機能性三尖弁閉鎖不全症 (FTR) 症例では造影 CT で三尖弁複合体にどのような形態学的変化が認められるかを検討した. 心臓大血管手術術前患者 45 例に対し造影 CT 及び経胸壁エコーを施行した. 造影 CT で拡張期及び収縮期の三尖弁輪面積, 三尖弁輪周囲長, 右心室容積, 先端間及び基部間における各乳頭筋間距離を計測した. 経胸壁心エコーによる TR grade ごと 4 群に分け (None + Trivial 群：26 例, Mild 群：6 例, Moderate 群：6 例, Severe 群：7 例), 各項目の有意差の有無及び, TR grade との相関関係を評価した. 群間で有意差を認めた項目 ($p>0.05$) は三尖弁輪面積 (拡張期, 収縮期) , 三尖弁輪周囲長 (拡張期, 収縮期) , 右心室容積 (拡張期) ,先端間前-後乳頭筋間距離 (拡張期, 収縮期) であった. TR grade と相関関係を認めた項目 ($r > 0.40$) は三尖弁輪面積 (拡張期, 収縮期) , 三尖弁輪周囲長 (拡張期, 収縮期) , 右心室容積 (拡張期, 収縮期) ,先端間前-後乳頭筋間距離 (拡張期, 収縮期) であった. 中隔乳頭筋については約 1/3 (35.6%) の症例で同定できず, 前乳頭筋, 後乳頭筋は全例で同定可能であったため, 前-後乳頭筋間距離のみが有効に計測することができた. 造影 CT で計測した三尖弁輪面積, 三尖弁輪周囲長, 右心室容積, 先端間前-後乳頭筋間距離は経胸壁心エコーによる TR grade と正の相関を示した. 造影 CT で機能性三尖弁閉鎖不全症の詳細な形態学的評価が可能であった.

NOTES

Conflicts of interest.— None declared.

Funding.— No funding was received for this work.